



Contents lists available at ScienceDirect

## Science of the Total Environment

journal homepage: [www.elsevier.com/locate/scitotenv](http://www.elsevier.com/locate/scitotenv)

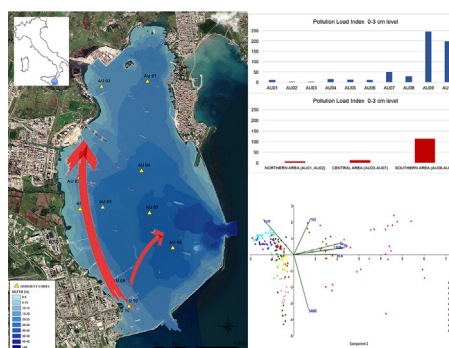
# Measuring anthropogenic impacts on an industrialised coastal marine area using chemical and textural signatures in sediments: A case study of Augusta Harbour (Sicily, Italy)

E. Romano<sup>a,\*</sup>, L. Bergamin<sup>a</sup>, I.W. Croudace<sup>b</sup>, G. Pierfranceschi<sup>c</sup>, G. Sesta<sup>c</sup>, A. Ausili<sup>a</sup><sup>a</sup> ISPR - Institute for Environmental Protection and Research, National Centre for Environmental Characterization and Protection of the Marine Coastal Areas, Via V. Brancati 60, Rome, Italy<sup>b</sup> GAU-Radioanalytical Laboratories, University of Southampton, National Oceanography Centre, European Way, Southampton SO14 3ZH, UK<sup>c</sup> ISPR, Institute for Environmental Protection and Research, National Laboratory Centre, Via di Castel Romano 100, Rome, Italy

## HIGHLIGHTS

- Coupled chemical-textural study of sediments optimized environmental information
- Sediments of Augusta harbour are affected by contamination legacy
- Sediments of the southern area were recognised as active source of secondary contamination
- Contaminant distribution patterns involving the whole harbour area were identified
- The harbour is a contaminant trap for increased fine sedimentation after the closure of the bay

## GRAPHICAL ABSTRACT



## ARTICLE INFO

## Article history:

Received 27 July 2020

Received in revised form 22 September 2020

Accepted 25 September 2020

Available online xxxx

Editor: Julian Blasco

## Keywords:

Mercury, barium and PCB/HCB polluted sediment

Particle-size indication of hydrodynamic isolation

Augusta Harbour

Contaminant distribution pattern

## ABSTRACT

From the early 1950s until the late 1970s, Augusta Bay (Sicily, Italy) served as a major European (petro) chemical hub. It thereafter began a progressive decline as several crude oil refining and industrial plants closed due to the transfer of production cycles to other sites around the globe. As a result of the rapid and relatively uncontrolled post-WWII development of the site, several environmental studies identified significant contamination in sediments around the southernmost sector of the bay. The pollution was mainly due to barium (Ba) and mercury (Hg), attributable to the former chlor-alkali plant (1958–2003), and polychlorobiphenyls (PCBs) and hexachlorobenzene (HCB). The present study focuses on understanding the broad legacy of pollution across the whole harbour by systematically analysing 10 sediment cores collected in 2008 for contaminant concentration profiles of Hg, Ba, PCBs, HCB and grain-size variations. Pre-industrial environmental geochemical background conditions were identified using data from the deeper parts of cores. The results show that contamination has affected the entire harbour area to varying degrees, and this has allowed identifying contamination transfer, based on decreasing concentrations and related depths in the sediment cores from the southernmost sector to the central and northern area. A recent finding by the current researchers is that the construction of the dam/breakwater in the early 1960s, that largely coincided with the start of industrial inputs, led to the trapping of fine terrestrial sediment inside the harbour, particularly in the central and northern area. This trapped sediment provides a granulometric time marker in those cores. The presence of highly contaminated sediments inside the harbour represents a significant future liability unless remedial action is applied to remove the worst of the polluted sediment.

© 2020 The Author(s). Published by Elsevier B.V. This is an open access article under the CC BY-NC-ND license (<http://creativecommons.org/licenses/by-nc-nd/4.0/>).

\* Corresponding author.

E-mail address: [elena.romano@isprambiente.it](mailto:elena.romano@isprambiente.it) (E. Romano).

## 1. Introduction

In the last century, many marine coastal areas have been subjected to strong disturbances that have altered their natural environments (Crain et al., 2009). These impacts have arisen from a combination of the effects of inadequate environmental legislation and monitoring, inputs from multiple leakages/discharges of industrial activities (e.g. chemical, petrochemical, thermoelectric, nuclear), uncontrolled landfills, intensive agricultural activities, military arsenals, shipyards and high maritime traffic. When the many associated contaminants flow into the aquatic environment, they become incorporated into marine and transitional sediments, interacting with biota and entering the human trophic chain (Reynoldson, 1987; Tessier and Campbell, 1988).

The development of Augusta Bay was seen as an opportunity to help Italian industry after WWII. Initially, petrochemical and chemical industries occupied the southern part of the bay and later a large breakwater/dam was constructed to enclose the bay and provide a safe refuge for shipping. It was recognised that the hydrodynamic isolation of the bay could allow for the trapping of polluted sediment, determining a secondary source of contamination. This situation could arise if the composition of the overlying surface waters changed (e.g. pH and complexing agents) or when sediments are brought from anoxic to the oxic environment such as during dredging activities (Salomons et al., 1987).

It is well-established that undisturbed accreting marine sediments provide an excellent archive of past natural and anthropogenic environmental changes because they preserve both records of varying chemical inputs and change of texture and mineralogical composition as a result of physical modification of sedimentary supply and distribution (Covelli et al., 2006; Apitz et al., 2009). For this reason, sediment cores from contaminated areas are used to investigate the temporal trends of contamination, recognising the extent of anthropogenic enrichment by comparison of levels deposited during the 'industrial period' with ancient unpolluted levels representing pre-industrial background conditions (Ontiveros-Cuadras et al., 2019; Ruiz-Fernández et al., 2019; Yang et al., 2020, among the most recent studies). In contaminated areas, vertical concentration profiles of contaminants are generally characterised by stable, lower concentrations in ancient sediments, representing local background values, and higher concentrations in the upper core levels (Matschullat et al., 2000; Birch, 2016). However, the anthropogenic impact on marine coastal areas may not be limited to the supply of contaminants but may alter the conditions of the sedimentary environment due to the possible establishment of multiple facilities in coastal areas (e.g. industries, harbours, urban centres). The consequent textural variation (grain size distribution) may exert control on the accumulation of contaminants (A. Wang et al., 2020) and, although not responsible for the degradation of environmental quality, it may be considered a proxy of the anthropogenic impact on marine sediments, assisting in the interpretation of chemical profiles (De Falco et al., 2004; Benmoussa et al., 2018; R. Wang et al., 2020). Consequently, an integrated chemical and sedimentological study of sediment cores, interpreted in the light of the chronology of human activities, offers a reliable tool for the historical reconstruction of anthropogenic impact on marine coastal areas.

An examination of sediment inputs into a changing hydrodynamic regime is potentially suitable for enclosed and low-energy settings, where moderate sedimentation rates provide detailed (high resolution) records of temporal changes. These environments may also be more affected by contamination than other coastal settings, because of the fine-grained sedimentation, which favours the accumulation of contaminants; moreover, they also act as pollutant-traps. In the last two decades, studies on dated sediment cores used for the reconstruction of contamination trends and sources were successfully conducted in semi-enclosed bays (Moon et al., 2009), lagoons (Zourarah et al., 2007) and harbours (Buckley et al., 1995; Owen and Sandhu, 2000; Tanner et al., 2000; Huerta-Díaz et al., 2008; Tang et al., 2008; Rodenburg and Ralston, 2017).

Several important Italian industrial centres, including mainly chemical and petrochemical plants, are located on the coast, often directly connected with large harbours. These activities exerted a strong impact in terms of extent, history, type and degree of contamination on the facing marine areas, which are characterised by high natural complexity and diversity. For this reason, the Italian Government recognised them as Sites of National Interest (SINs) and planned an adequate environmental characterisation for the successive reclamation project (Ausili et al., 2020). Among these sites, Augusta Bay (eastern Sicily) is of particular interest mainly because of the presence of a large petrochemical complex, which has exerted a strong anthropogenic impact on the facing marine area and the related environmental matrices (Sciaccia and Fallico, 1978; ICRAM, 2008; Romano et al., 2009; Sprovieri et al., 2011; Bellucci et al., 2012; Bonsignore et al., 2013; Di Leonardo et al., 2014; Croudace et al., 2015; Romano et al., 2016).

The aim of this research was to compare the contaminant levels (considered a legacy of past industrial activities) to the potential contamination resulting from specific industrial processes active in the area, and sediment textural variations in 10 cores, collected across the whole harbour system. The study was informed by previous knowledge of contamination sources. The timing of contamination inputs will improve our understanding of the spatial and temporal distribution of pollution and sedimentation patterns.

## 2. Study area

Augusta Bay is a natural embayment 8 km long and 4 km wide (Fig. 1), bordered by breakwaters built in the early 1960s. The territory behind the harbour is characterised geologically by Meso-Cenozoic carbonates and basalts of the Hyblean plateau outcropping on the mainland, and Pliocene clays and Quaternary biocalcarenes along the coast (Carbone, 2011). The marine area is a micro-tidal system characterised by poor water circulation, with a main and weak hydrodynamic cell in the central-southern harbour moving 5–6 cm s<sup>-1</sup> and alternating directions according to specific tide conditions (ICRAM, 2008; Feola et al., 2016). Some sediment re-mobilisation may occur due to shipping activity, but the preservation of sedimentary chronological records suggests that these effects are not pronounced.

Augusta Harbour is characterised by intense commercial and industrial maritime activity as well as the presence of a huge chemical and petrochemical complex, which has been in operation for several decades. The industrial activities started in the 1950s and quickly developed until the 1980s, making the site the most important hub in Europe. Subsequently, some industries closed, while others are still active. In particular, a mercury-cell chlor-alkali plant operated from 1958 to 2003 and was considered a major environmental concern for the marine area due to the discharge into the sea of over 500 tons of mercury (Hg) during a period in history when environmental legislation was inadequate (Croudace et al., 2015; Ausili et al., 2020).

The intense and long-lasting industrial activity has left a heavy pollution legacy on the terrestrial and marine environment. A large and extended environmental characterisation of the marine area carried out in 2005 by ICRAM (2008), showed exceptionally high concentrations, mainly located in the southern sector, of Hg, up to 198 mg kg<sup>-1</sup> in the surface samples and to 728 mg kg<sup>-1</sup> in the deeper ones. Very high levels of barium (Ba), hexachlorobenzene (HCB) and polychlorobiphenyls (PCBs), up to 1320 mg kg<sup>-1</sup>, 0.18 mg kg<sup>-1</sup> and 0.83 mg kg<sup>-1</sup>, respectively, were found in the surface samples. Similar results were obtained by Romano et al. (2009, 2013) who determined in superficial sediments of the southern area significant contamination due to Hg, PAHs and PCBs (up to 321 mg kg<sup>-1</sup>, 19.50 mg kg<sup>-1</sup> and 3.75 mg kg<sup>-1</sup>, respectively). Several other studies reported major contamination of marine sediments in the Augusta Harbour (Sciaccia and Fallico, 1978; Sprovieri et al., 2011; Bellucci et al., 2012; WHO, 2012; Croudace et al., 2015; Salvaggio Manta et al., 2016; Tamburrino et al., 2020). Finally, Croudace et al. (2015), dated 3 sediment cores using radiometric methods

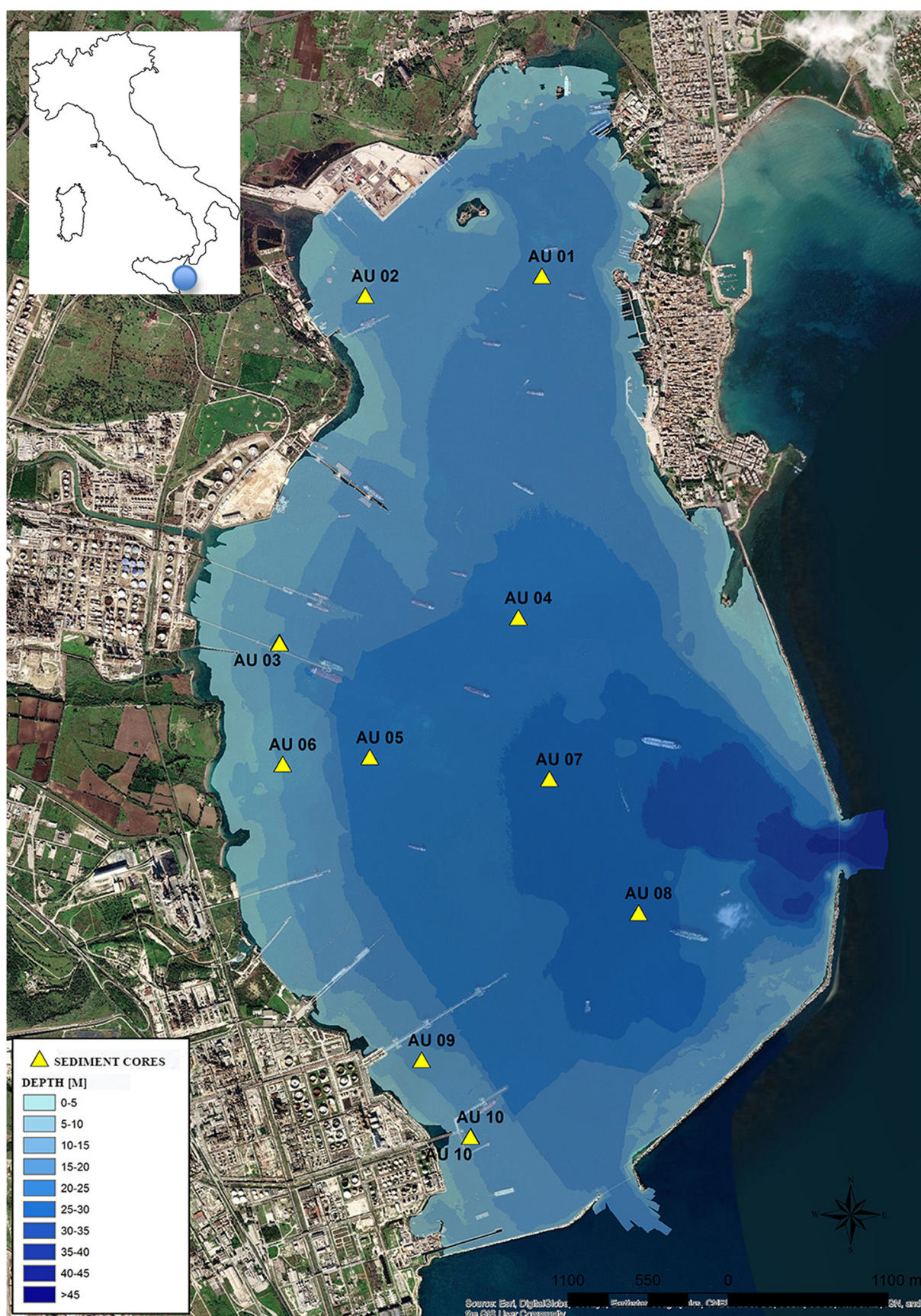


Fig. 1. The semi-enclosed Augusta Bay study area showing sediment sampling stations.

( $^{137}\text{Cs}$ ), reconstructed the contamination chronology and showed that the exceptionally high concentrations of Hg and Ba were attributable to the historical activity of the chlor-alkali plant while PCBs were likely derived from petrochemical plants. Additionally, high Hg content, exceeding the regulatory limits for food consumption (CE regulation 1881/2006), were found in tissues of fish and mussels collected from the Bay (Ausili et al., 2008; ICRAM, 2008; Bonsignore et al., 2013; Signa et al., 2017).

### 3. Materials and methods

Considering previously obtained information about the study area, this research focused on the study of concentration profiles of Hg, Ba, HCB and PCBs as the sum of the following congeners: 28, 52, 77, 81, 101, 105, 114, 118, 123, 126, 128, 138, 153, 156, 157, 167, 169, 170, 180, 189 and 209, in 10 sediment cores from Augusta Harbour (Table 1). Sediment grain-size was also considered for the interpretation of chemical data and as a proxy of anthropogenic impact.

#### 3.1. Sampling

The sampling scheme was planned based on results from an earlier in-depth characterisation (ICRAM, 2008) and considering the water circulation patterns in the harbour (Lisi et al., 2009). Particular care was taken by using bathymetric and seismic surveying (ICRAM, 2008) to avoid collecting disturbed cores in areas where shipping or dredging activities could have impacted the sediment record. The 10 sediment cores were collected in 2008 by gravity corer SW 104 Carma® equipped with an internal HDPE liner. This device was designed to retain the sediment-water interface, and no significant differences were recognised in sediment compositional data obtained using a vibrocorer; this indicates that sediment compaction and potential downward drag of the contaminants was limited (Magagnoli and Mengoli, 1995; Romano et al., 2018a). Each core was sub-sampled by extrusion to provide samples for determination of grain size, qualitative mineralogy and chemical concentrations. For this purpose, incremental samples at 3 cm intervals were collected: 10 sub-samples were continuously taken in the first 30 cm of the core, providing the highest resolution for recent material, while 1 sub-sample every 10 cm was collected from -30 cm to the core bottom to detect the main environmental changes in earlier periods. This scheme allowed for a detailed investigation of the upper contaminated levels, while it analyses the ancient unpolluted sediments without wasting sample material. Each sub-sample was homogenised and then split into 3 separate aliquots for the analysis of grain-size (including the qualitative mineralogical study), trace and major elements and organic contaminants.

#### 3.2. Grain-size and chemical analysis

Grain-size analyses were conducted according to Romano et al. (2018b) on pre-treated samples, successively wet-separated into coarse (> 63  $\mu\text{m}$ ) and fine (< 63  $\mu\text{m}$ ) fractions. The coarse fraction was dry-

sieved with meshes (ASTM series) ranging from -1 to +4  $\phi$ . The fine fraction was analysed using a laser granulometer (HELOS FKV, Sympatec, Germany) after being placed into a dispersant solution of sodium hexametaphosphate. Results from the analysis of coarse and fine fractions were integrated utilising specific software to obtain the comprehensive distribution curve, ranging from -1 to +10.5  $\phi$ . The >63  $\mu\text{m}$  fraction was also examined under a stereomicroscope (Leica M205C up to 120x) for a qualitative analysis of the main inorganic and organic sediment components. The analysis consisted of the identification of the main elements of the abiotic (minerals and lithic fragments) and biotic (bioclasts) components finalised to identify potential sedimentary sources. Minerals were identified based on their crystalline habit, colour, hardness, reactivity to hydrochloric acid, and response to a magnet. Sediments were then classified according to Shepard (1954).

Samples for determination of Ba and Hg, previously dissolved using microwave-assisted digestion (Milestone MLS Ethos TC high-performance microwave digestion unit) with 3 mL of  $\text{HNO}_3$  and 9 mL of superpure HCl, were analysed according to the methods described by Bergamin et al. (2009). Ba was then measured using ICP-OES (Liberty AX) while Hg through a Milestone Direct Mercury Analyzer (DMA-80). The used CRMs (Certified Reference Material) were PACS-2 e MESS-3 certified by National Research Council of Canada; the quantification limit (LOQ) was 1  $\text{mg kg}^{-1}$  d.w. for Ba and 0.0005  $\text{mg kg}^{-1}$  d.w., for Hg.

PCBs and HCB were analysed according to Bergamin et al. (2009) as <2 mm homogenised, freeze-dried samples and then subjected to pressurised fluid extraction using a Dionex model ASE 200 extractor with 60:40 Petroleum ether/dichloromethane solvent mixture. The determination was performed by high-resolution gas chromatography with electron capture detection (GC/ECD) in dual column dual detector mode. The method was initially tested on certified reference materials (NIST 1941B and NIST 1944) that were successfully analysed (recovery values were, respectively, in the 65%–112% and 61%–97% range for the analytes with certified values); the quantification limit was 0.0001  $\text{mg kg}^{-1}$  d.w.

For all chemical analyses, the quality control was tested through verification of a method blank, a spiked blank for recovery evaluation, sample replicates and CRMs on each extraction batch (see supplementary material). The uncertainty for Ba and Hg was <20% while <30% for PCBs and HCB.

#### 3.3. Statistical processing

A correlation matrix was obtained for each core using the non-parametric Spearman's index ( $\rho$ ) for highlighting possible correlations between pairs of contaminants and sediment fractions (sand, silt and clay). Principal component analysis (PCA) was conducted on the whole dataset of chemical results after z-score standardisation. Statistical analysis was carried out using the PALaeontological STatistics-PAST package, ver. 3.18 (Hammer et al., 2001).

## 4. Results

#### 4.1. Sediment grainsize and mineralogy

All results of grain size analysis, as percentages of sand, silt, and clay, are given in Supplementary Materials and are graphically summarised in Fig. 2. Along the depth of the AU01 and AU04 cores, a similar prevalence of silt and clay (~ 50%) was observed; the prevalence of sand was similar throughout the cores, while there was only a slight change of silt and clay, with a prevalence of clay in the upper sections. In AU02, AU03, AU05, AU07, and AU09, silt was always the prevailing fraction (~ 60%) over clay (< 40%) and sand (> 10%). The textural variability along the entire depth was the highest in AU03, moderate in AU02, AU09 and AU07, and low in AU05. Core AU06 showed similar sand, silt and clay percentages in the upper 60 cm, while sand increased to

**Table 1**  
Details on sediment sampling stations.

Station	Y UTM WGS84	X UTM WGS84	Water depth (m)	Core thickness (cm)
AU01	4120633	518617	17.6	116
AU02	4120498	517402	12.7	82
AU03	4118114	516813	10.2	81
AU04	4118283	518455	23.1	98
AU05	4117322	517433	23.0	63
AU06	4117274	516835	10.9	111
AU07	4117173	518669	27.1	105
AU08	4116252	519283	28.8	39
AU09	4115239	517790	12.4	104
AU10	4114715	518127	10.4	125

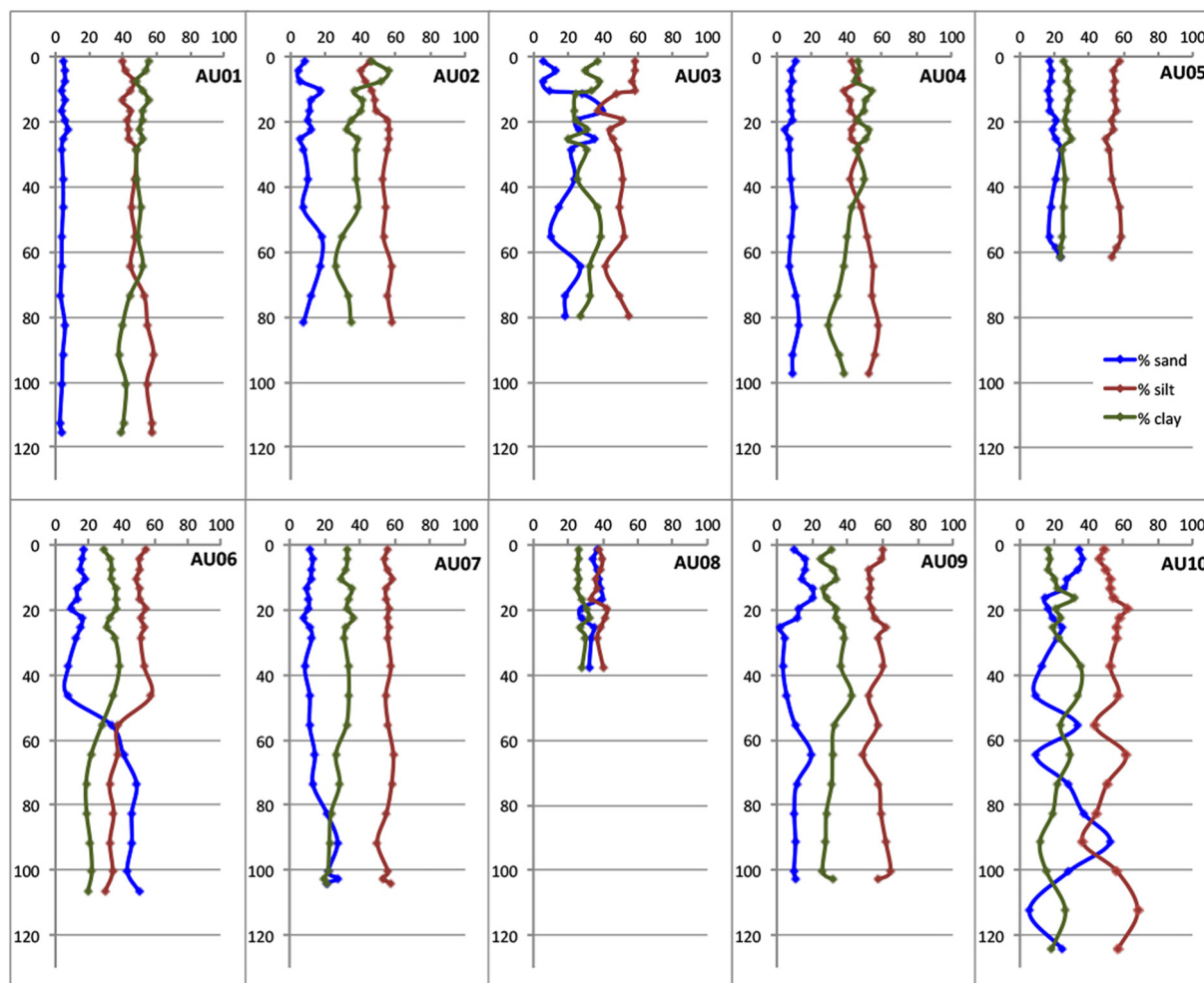


Fig. 2. Grain size profiles for sand, silt and clay percentages with depth (cm).

>40% in the deeper part. The short core AU08 displayed both sand and silt approximately between 30% and 40%; silt prevailed in the lower section, while sand was more abundant in the upper one; clay was steady between 25% and 30%. Core AU10 showed relatively constant silt content (~50%), although it showed the highest sand percentages and textural variability along the depth (Fig. 2).

The qualitative study of the >63  $\mu\text{m}$  fraction under the stereomicroscope showed, from almost all the examined levels, a predominant bioclastic composition, essentially shells, fragments of bivalves, gastropods, echinoids, bryozoans, porifers, annelids, ostracods and foraminifers associated with abundant vegetable frustules and earthy aggregates. The main minerals were quartz, feldspar, and calcite and carbonate lithic granules, biotite, pyroxenes and volcanoclastic fragments. In AU09 and

AU10 in particular diffuse anthropogenic granules (spherules from compact to spongy, from light orange to yellow; blackish residual granules, sometimes sub-rounded) were present in up to one-meter depth (Fig. 3). Residual blackish granules and coal fragments were frequently found in the first 50 cm of AU06, while they were sporadic and confined to the uppermost levels in all the other cores.

#### 4.2. Chemical analyses

Chemical results are reported in Supplementary Material and are graphically summarised in Figs. 4–7. To evaluate these data, local background concentrations (BGVs) for Ba and Hg were defined according to Romano et al. (2015). For this purpose, the uncontaminated levels of

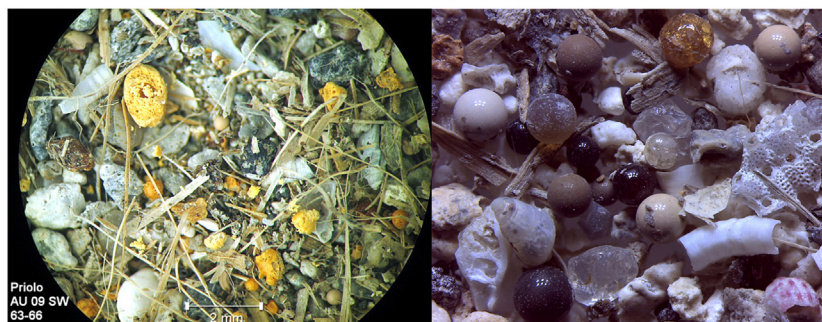


Fig. 3. Anthropogenic granules from core AU09 (left) and spherules in core AU10 (right) from the >63  $\mu\text{m}$  fraction.

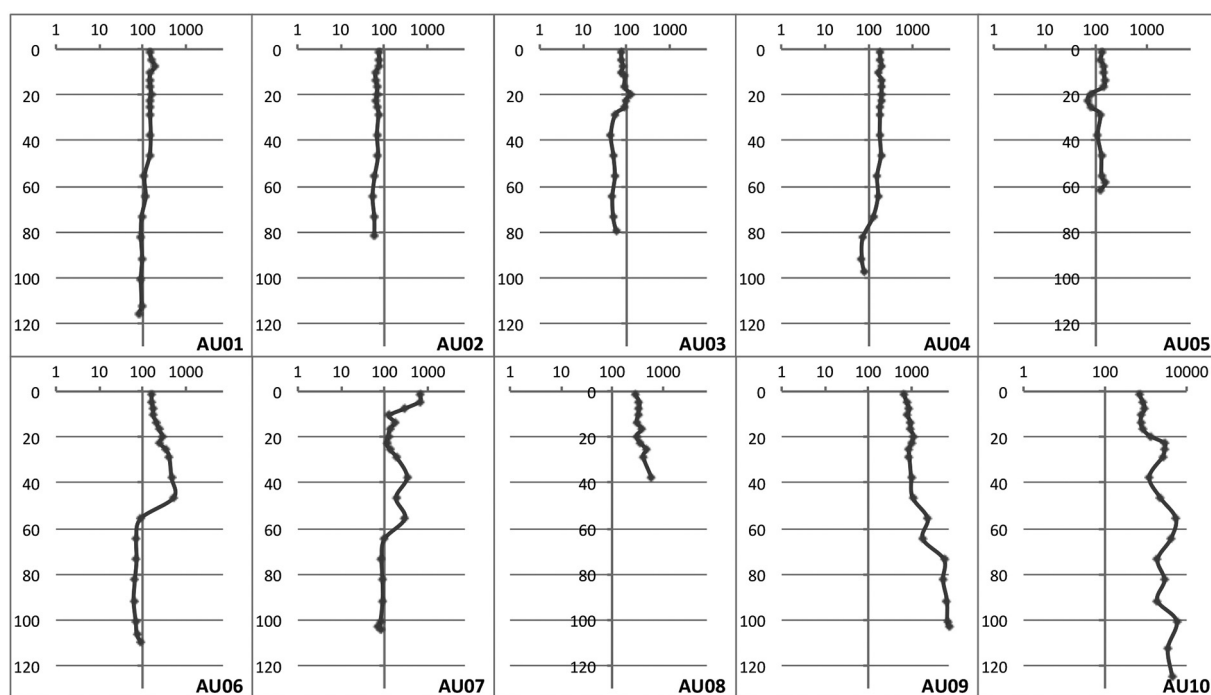


Fig. 4. Ba concentration ( $\text{mg kg}^{-1}$ ) profiles with depth (cm). The y-axis intercepts the x-axis at the BGV ( $105 \text{ mg kg}^{-1}$ ).

cores from areas not affected by dredging activities (AU01, AU02, AU03, AU06) were considered. These levels were detected comparing the Ba, Hg, PCBs and HCB concentration profiles and the sedimentation rate of AU02 ( $7 \text{ mm yr}^{-1}$ ) determined by Croudace et al. (2015), providing the depth below which the sediment is not affected by contamination. The BGVs were  $105 \text{ mg kg}^{-1}$  and  $0.28 \text{ mg kg}^{-1}$  for Ba and Hg, respectively.

#### 4.2.1. Barium results

AU02 and AU03 always displayed concentrations always below the BGV, except for a small peak of  $122 \text{ mg kg}^{-1}$  around  $-20 \text{ cm}$  in AU02. Cores AU01 and AU04 showed concentrations slightly exceeding BGV in the upper section ( $74\text{--}65 \text{ cm}$ ), while AU05 was slightly above BGV for the whole length ( $63 \text{ cm}$ ), except for an interval between  $-23$  and  $-19 \text{ cm}$ ; in these 3 cores, the highest concentrations of  $192 \text{ mg kg}^{-1}$ ,

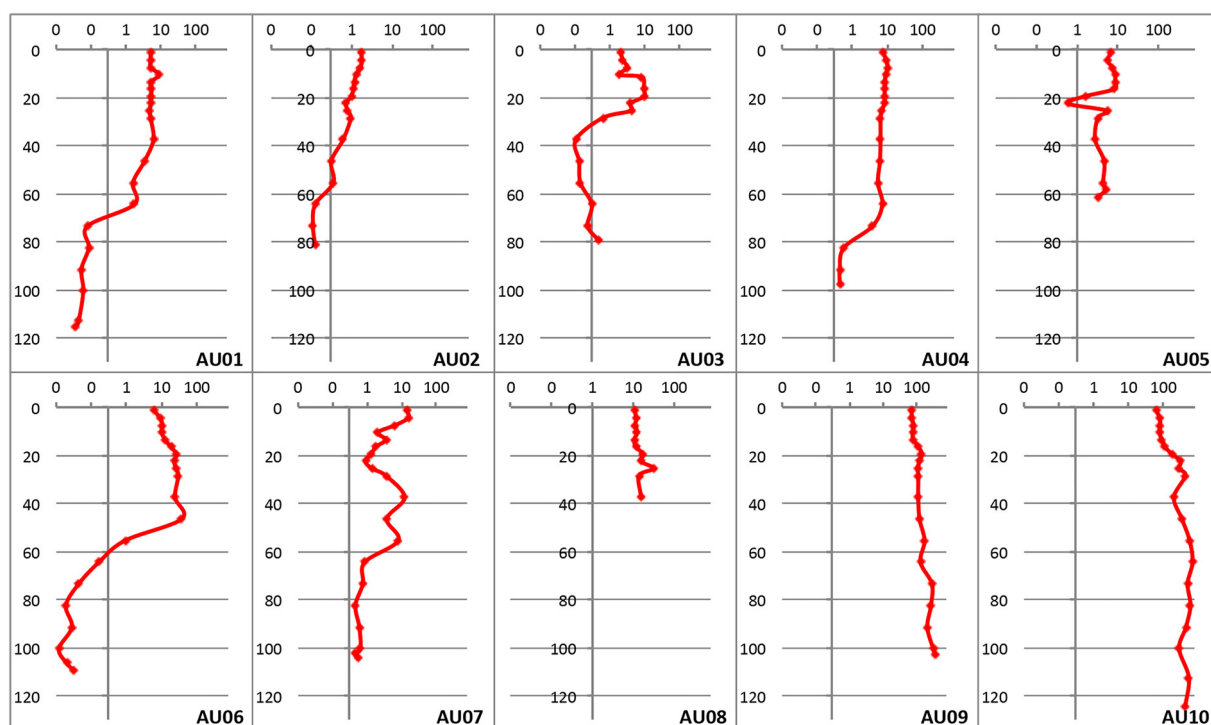


Fig. 5. Hg concentration ( $\text{mg kg}^{-1}$ ) profiles with depth (cm). The y-axis intercepts the x-axis at the BGV ( $0.28 \text{ mg kg}^{-1}$ ).

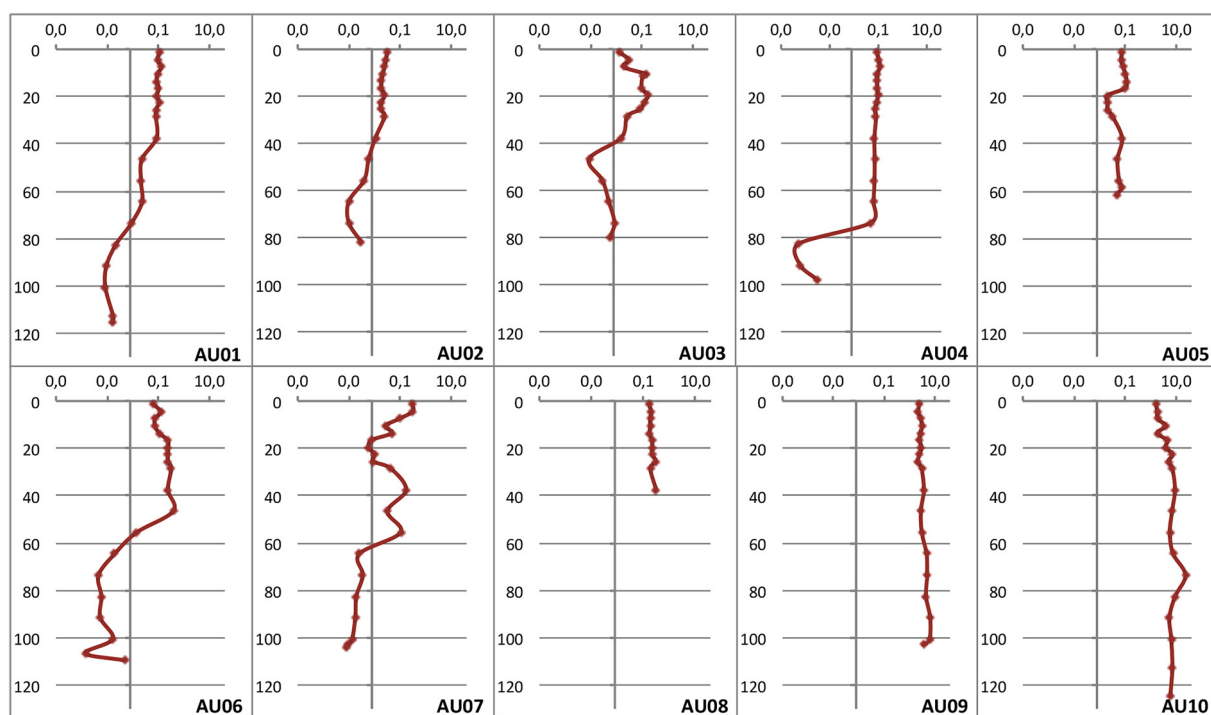


Fig. 6. PCBs concentration ( $\text{mg kg}^{-1}$ ) profiles with depth (cm). The y-axis intercepts the x-axis at EQS. ( $0.008 \text{ mg kg}^{-1}$ ).

201  $\text{mg kg}^{-1}$  and 155  $\text{mg kg}^{-1}$  were recorded at  $-8 \text{ cm}$  in AU01,  $-14 \text{ cm}$  in AU04 and  $-65 \text{ cm}$  in AU05, respectively. Cores AU06 and AU07 showed very high concentrations in the upper section, 47 and 56  $\text{cm}$  thick respectively, while they were constant and lower than BGV in the lower section; the highest value of 521  $\text{mg kg}^{-1}$  was

recorded at  $-47 \text{ cm}$  for AU06 and of 677  $\text{mg kg}^{-1}$  at  $-2 \text{ cm}$  for AU07. Core AU08, which was too short to reach the lower uncontaminated levels, displayed a pattern very similar to AU06, with the highest concentration of 587  $\text{mg kg}^{-1}$  at the bottom ( $-38 \text{ cm}$ ). Finally, AU09 and AU10 showed exceptionally high concentrations along the whole core,

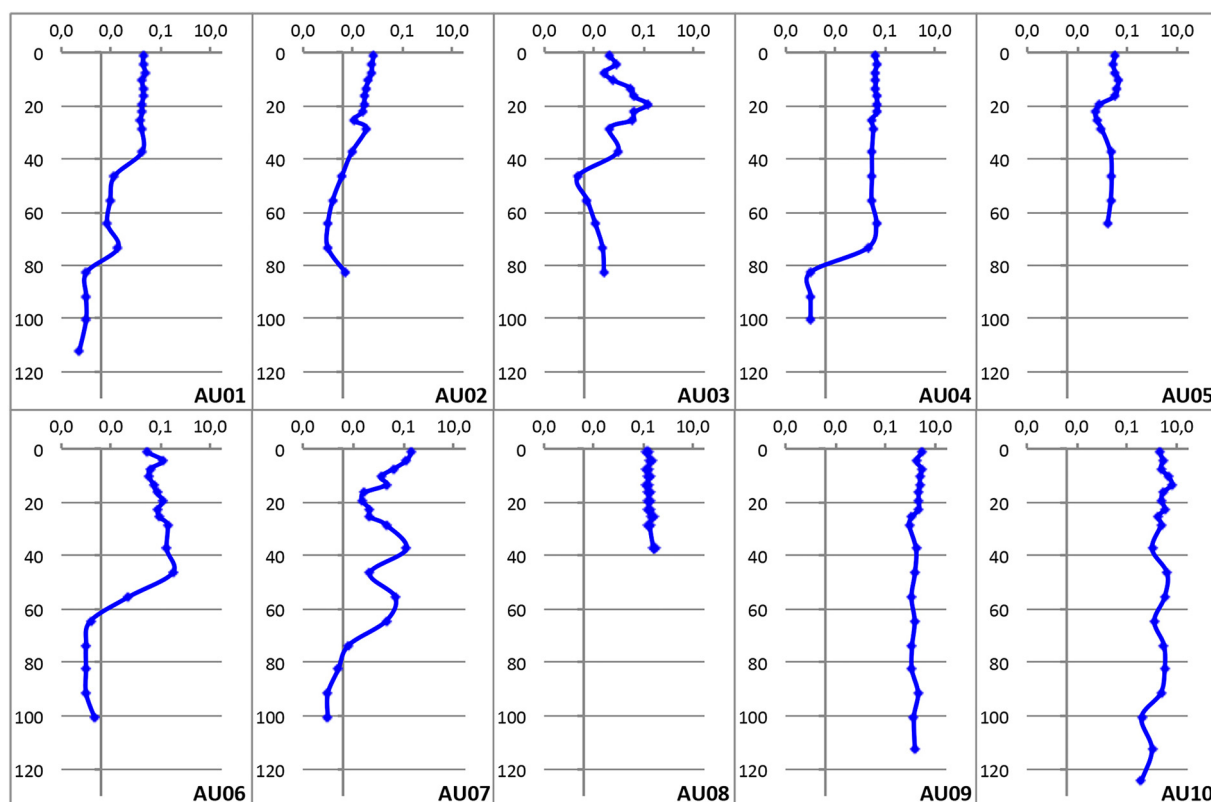


Fig. 7. HCB concentration ( $\text{mg kg}^{-1}$ ) profiles with depth (cm). The y-axis intercepts the x-axis at EQS. ( $0.0004 \text{ mg kg}^{-1}$ ).

even though they were the longest cores. The highest value for AU09 was  $7199 \text{ mg kg}^{-1}$  at the core bottom ( $-125 \text{ cm}$ ), while for AU10 it was  $5708 \text{ mg kg}^{-1}$  at  $-101 \text{ cm}$ . Concentrations generally decreased upwards in both cores, while maintaining very high values (Fig. 4).

#### 4.2.2. Mercury results

The sediment cores AU01, AU02 and AU06 were characterised by moderately variable concentrations always above the BGV at a similar depth range from  $56$  to  $65 \text{ cm}$ ; below, values decreased and were more uniform. However, the degree of contamination in these cores was considerably different: the highest concentration in AU01 was  $9.03 \text{ mg kg}^{-1}$  at  $-11 \text{ cm}$ , in AU02  $1.79$  at  $-5 \text{ cm}$ , and in AU06,  $37.16 \text{ mg kg}^{-1}$  at  $-47 \text{ cm}$ . Core AU03 displayed a similar pattern, although the increase in Hg started at considerably shallower level ( $-30 \text{ cm}$ ), decreasing after a peak ( $10 \text{ mg kg}^{-1}$  at  $-8 \text{ cm}$ ), in the upper levels. Cores AU04, AU05, and AU07 showed Hg concentrations above BGV for their entire length, with maximum values in the upper  $15 \text{ cm}$  of  $10.18 \text{ mg kg}^{-1}$ ,  $8.70 \text{ mg kg}^{-1}$  and  $15.42 \text{ mg kg}^{-1}$ , respectively. AU08 had a maximum of  $31.12 \text{ mg kg}^{-1}$  at  $-26 \text{ cm}$ . Cores AU09 and AU10 showed exceptionally high concentrations along the whole length, up to  $342.31 \text{ mg kg}^{-1}$  at the core bottom ( $-113 \text{ cm}$ ) and up to  $680.10 \text{ mg kg}^{-1}$  at  $-65 \text{ cm}$ , respectively, showing a general decreasing pattern from the bottom to the top even though the values remained very high (Fig. 5).

#### 4.2.3. PCBs results

For the evaluation of PCBs concentration, the Environmental Quality Standard (EQS), defined as per Directive 2000/60/EU as criteria for achieving Good Chemical and Ecological Status of coastal areas, and established ( $0.008 \text{ mg kg}^{-1}$ ) by the Italian regulation (Legislative decree 172/2015), was considered. Most cores (AU01, AU02, AU03, AU04, AU06, and AU07) showed an upper contaminated section, of variable thickness (from  $38 \text{ cm}$  in AU02 and AU03 to  $74 \text{ cm}$  in AU04), and a lower section with concentrations close to zero; maximum values were between  $0.032 \text{ mg kg}^{-1}$  in AU02 and  $0.386 \text{ mg kg}^{-1}$  in AU06. In these cores, the highest concentrations were found in the upper  $20 \text{ cm}$ , except for AU06, where it was recorded at  $-47 \text{ cm}$ . AU03 was the only core with a marked decrease, down to  $0.014 \text{ mg kg}^{-1}$  at the core top. The shortest cores, AU05 and AU08, were contaminated for their entire lengths, with the highest value of  $0.114 \text{ mg kg}^{-1}$  and  $0.309 \text{ mg kg}^{-1}$  at  $-14$  and  $-38 \text{ cm}$ , respectively. AU09 and AU10 demonstrated exceptionally high concentrations along the entire cores, up to  $5.031$  and  $22.988 \text{ mg kg}^{-1}$ , both at  $-74 \text{ cm}$ , respectively, with a general decreasing pattern from the bottom to the top while maintaining very high values (Fig. 6).

#### 4.2.4. HCB results

For the evaluation of HCB concentrations, the EQS of  $0.0004 \text{ mg kg}^{-1}$  was considered. Most cores (AU01, AU02, AU04, AU06, AU07) showed an upper contaminated section and a lower one where HCB was virtually absent (Fig. 7). Different thicknesses of contaminated sediment were measured in these cores:  $38 \text{ cm}$  for AU02,  $56 \text{ cm}$  for AU06,  $65 \text{ cm}$  for AU07 and  $74 \text{ cm}$  for AU01 and AU04. Maximum concentrations were found in the upper  $20 \text{ cm}$  and ranged between  $0.0007 \text{ mg kg}^{-1}$  in AU02 and  $0.0507 \text{ mg kg}^{-1}$  in AU04. Core AU03, although also characterised by a more contaminated upper section, with a maximum of  $0.115 \text{ mg kg}^{-1}$  at  $-20 \text{ cm}$ , displayed concentrations above EQS also in the lower section. The shortest cores AU05 and AU08 were contaminated for the entire length, with rather steady values and highest concentrations of  $0.0455 \text{ mg kg}^{-1}$  and  $0.2608 \text{ mg kg}^{-1}$  at  $-11$  and  $-38 \text{ cm}$ , respectively. AU09 and AU10 demonstrated exceptionally high concentrations along the whole core; in the former, values ranged between  $0.8999 \text{ mg kg}^{-1}$  at  $-29 \text{ cm}$  and  $2.9634 \text{ mg kg}^{-1}$  at the core top, while in the latter, they ranged between  $0.3844 \text{ mg kg}^{-1}$  at the core bottom ( $-124 \text{ cm}$ ) and  $6.3059 \text{ mg kg}^{-1}$  at  $-14 \text{ cm}$ .

## 5. Discussion

### 5.1. Distribution of contaminants in Augusta Harbour

Concentration profiles for Ba, Hg, PCBs and HCB in the investigated cores showed significant variation in different harbour sectors. However, while contamination due to Ba (existing as anthropogenic barite; Croudace et al., 2015) was absent in the northern sector (AU01 and AU02) and the central coastal one (AU03), for all the other contaminants there was significant variability of contamination levels across the entire area. In order to compare the degree of contamination for all the parameters, the Contamination Factor (CF) was used. It was determined according to Muthu Raj and Jayaprakash (2008) as the ratio between sample concentration and BGVs and EQS for heavy metals and organic contaminants, respectively (Fig. 8). Considering the 4 CF categories ( $< 1$  uncontaminated,  $1-3$  moderate contamination,  $3-6$  considerable contamination and  $> 6$  very high contamination), with regards to Ba, AU02 was uncontaminated (CF max  $0.7$ ), AU01, AU03, AU04 and AU05 were moderately contaminated (CF max  $1.2-1.8$ ), and AU06 and AU08 were considerably contaminated (CF max  $5.0-5.6$ ). AU07, AU09 and AU10 were very highly contaminated, with considerable difference between AU07 (CF max  $6.5$ ) (CF max  $6.5$ ) and the latter two (CF max  $68.6$  and  $54.4$  in AU09 and AU10, respectively). Concerning the other contaminants, all sediment cores were highly contaminated (CF  $> 6$ ), except for AU02, which was, at most, considerably contaminated with PCBs (CF max  $4.0$ ). The highest CF for Ba was  $69$  in AU09, while Hg, PCBs and HCB all had the highest CFs ( $2,429$ ,  $2,873$  and  $15,765$ , respectively) all in core AU10.

These pollution levels were compared to those of other highly industrialised areas. The Victoria Harbour (Hong Kong), is the world's busiest container port with a strong anthropogenic impact which has determined the alteration of coastline and uncontrolled disposal of industrially polluted wastes, especially from the mid-1950s to the present, resulting in seabed contamination. The most critical pollutant recognised in sediment cores was Cu, which was found enriched between  $3$  and  $312$  (Tanner et al., 2000). Surface sediments from the entire Hong Kong coastal zone were found to be anthropogenically enriched in heavy metals (mostly Cu) by at most approximately  $10$  (Zhou et al., 2007). A study carried out on sediments collected in the vicinity of a mercury cell chlor-alkali plant in Dalhousie (Canada), found Hg enriched at most  $15$  times with respect to local background concentration of  $0.07 \text{ mg kg}^{-1}$  (Garron et al., 2005).

The Pollution Load Index (PLI) for surface ( $0-3 \text{ cm}$ ) sediment layers at single sampling stations and for the northern, central and southern areas of the harbour (Fig. 9) was determined considering all the analysed parameters, according to Tomlinson et al. (1980) and Shen et al. (2019);  $\text{PLI} > 1$  indicated polluted sediments. Results clearly showed that a high degree of pollution affected the bottom sediments of the whole harbour area in 2008 with an evident decreasing trend from the southern to the northern area. On the whole, CF and PLI patterns suggested a redistribution of contaminants from the southern to the northern area through mechanisms still active at the time of sampling.

It was already demonstrated that, in studies based both on sediment cores and surface samples, multivariate statistical analysis was a powerful tool for identifying contaminants of common origin and their source (Chen et al., 2016; Gao et al., 2016) even if in the Augusta Harbour it was already recognised (Bellucci et al., 2012; Croudace et al., 2015). Nevertheless, in this study, PCA was used, associated with the correlation analysis (Yang et al., 2020), to evaluate the chemical and textural characteristics of the 10 analysed cores in a combined way, to assess their distribution among samples, highlighting the correlations existing among them.

In the scatter plot of the two first components (Fig. 10) all the contaminants align on PC1 representing the most important factors to explain the distribution of the samples; they are also strongly correlated

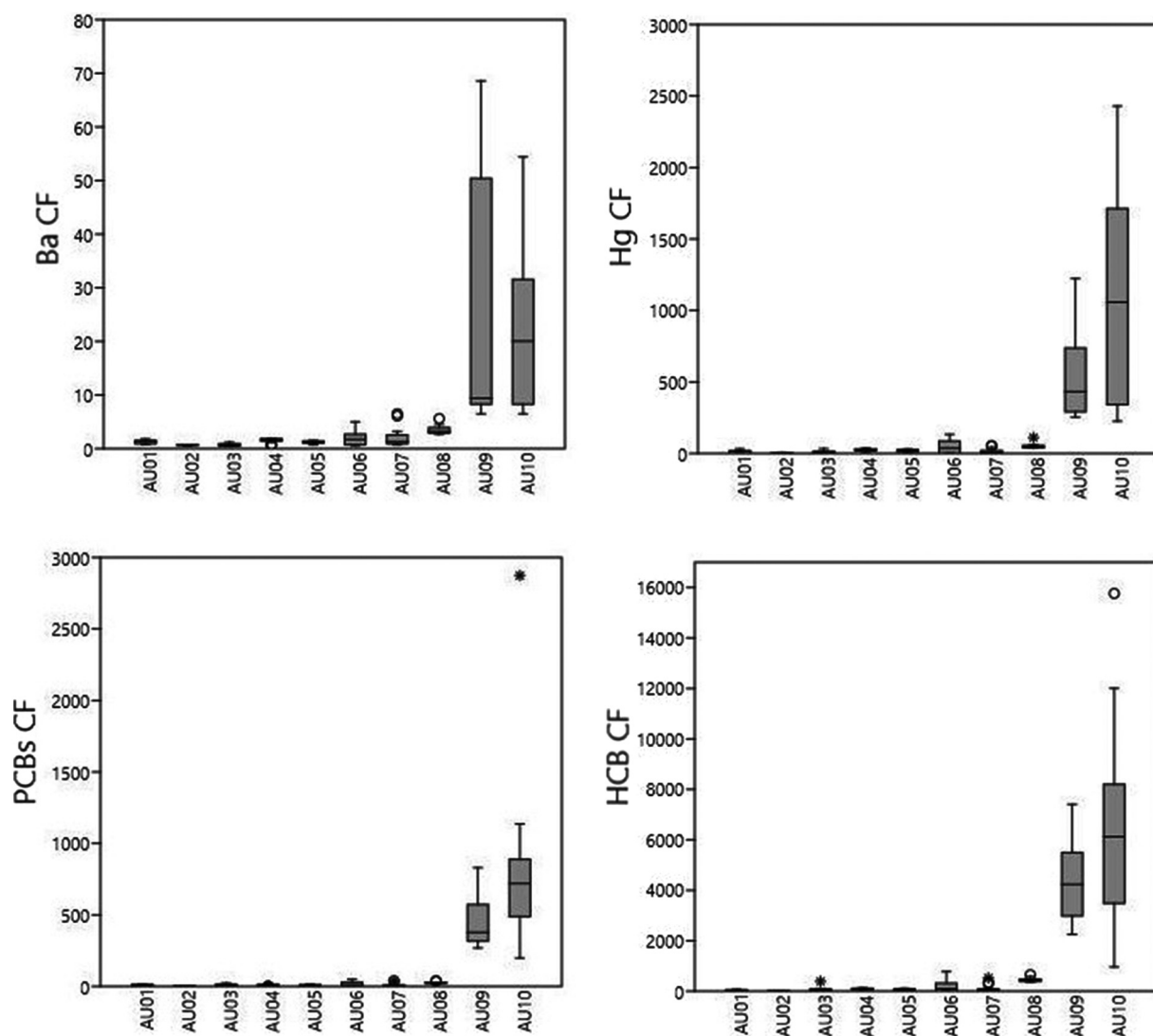


Fig. 8. Box and whisker plots of Contamination Factor in the different cores. Circles and dots represent outliers.

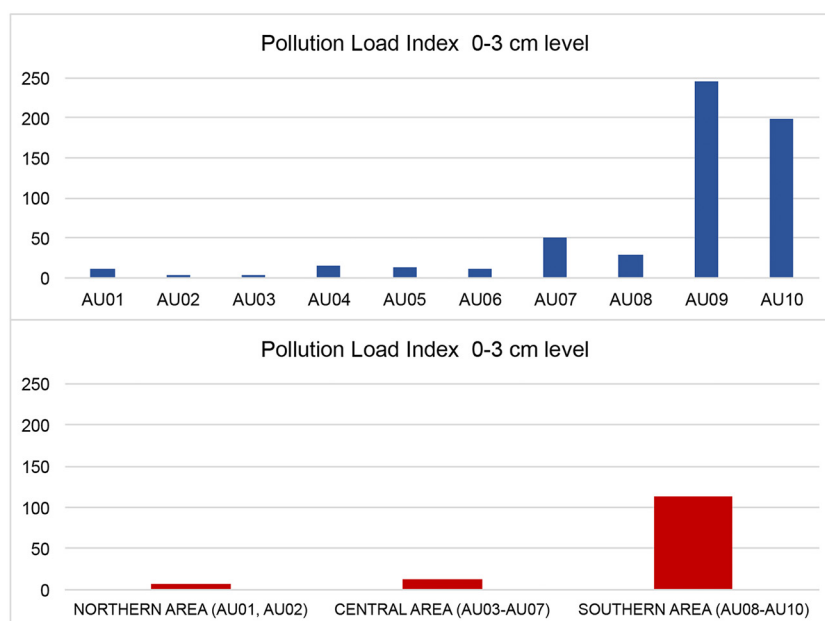
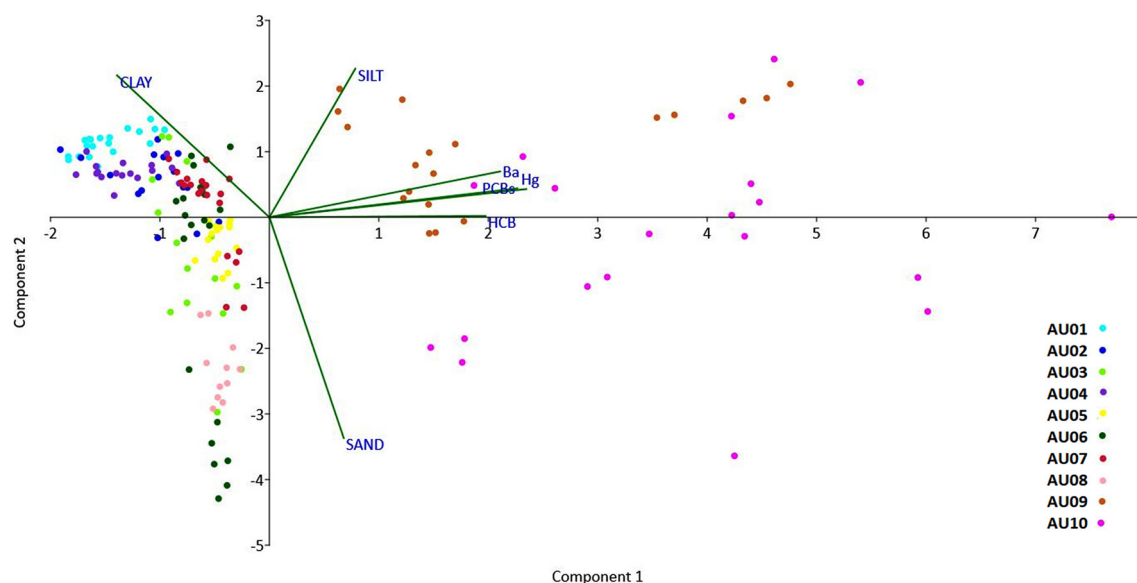


Fig. 9. Pollution Load Index determined for surface sediments (0–3 cm) at single sampling stations and for the three main areas of the harbour.



**Fig. 10.** Principal Component Analysis (PCA) applied on the whole dataset (grain size and chemical data). PC1 and PC2 account for 42% and 26% of the variance, respectively.

with each other, consistently with their common sources and anthropogenic origin. This result was also confirmed by the correlation matrix (Spearman's  $\rho$ ), which was applied to analytical results in each core (see Supplementary Material), highlighting significant correlations ( $p < 0.01$ ) between all contaminants, strongly indicating a common production process; the only exception was for HCB, which was not correlated with the other contaminants in AU09 and AU10. In the PCA, the correlation between contaminants and fine fractions (silt and clay) was not recognised because data from all the cores were processed together. In contrast, the correlation matrices applied to the single cores highlighted the inter-relationship of contaminants with clay, and in most cases with silt, except for AU03, AU09 and AU10 (see Supplementary Material). This result suggests the deposition of contaminants in association with fine sediments far from the source.

AU09 and AU10 samples had positive values of PC1, distributed over a wide range, while all the others have negative values in restricted intervals; this shows that these cores, compared to all the others, have much higher levels of contamination and are characterised by greater variability (Fig. 10). This result indicates a decreasing gradient of contamination starting from AU10 towards AU09 and subsequently towards all the other cores, placed on the negative side of the first component.

Cores AU09 and AU10 are the most contaminated by all pollutants throughout their depth and clearly indicate the industrial area as the main source of contamination. Several studies conducted on this site agreed on the identification of the chlor-alkali plant as the source of Hg, Ba and PCBs (Sprovieri et al., 2011; Bellucci et al., 2012; Romano et al., 2013; Croudace et al., 2015; Romano et al., 2016). In particular, Croudace et al. (2015) analysed replicates of the AU10 of the present work by means both of Itrax-CS and conventional WD-XRF determining sediment accumulation rates utilising  $^{137}\text{Cs}$  geochronology. The authors concluded that the chlor-alkali plant supplied Ba and Hg because the main changes in the concentration profiles agreed with the well-known chronology of events influencing the discharge of these contaminants (Fig. 11). In detail, the significant decrease of Hg concentration, starting at  $-60$  cm, was dated to approximately 1980 according to a sedimentation rate of  $2.6 \text{ cm yr}^{-1}$ , and attributed to the establishment of a demercurisation plant, while the further decrease at  $-20$  cm, corresponding to the late 1990s, was attributed to the end of production in the chlor-alkali plant (Fig. 11). These results are used to identify the origin and distribution patterns of contaminants, the highest concentrations of which occurred in the southernmost sector of the harbour

(AU09 and AU10) and affected the entire thickness of the cores with the highest concentration at the bottom. Starting from this area, there was a transport of contamination towards the other sectors of the harbour. In particular, in the shallower sector of the harbour (within 20 m water depth), a gradient from the southern area was identified, both in terms of concentration and thickness of contaminated sediment, towards the north (AU06, AU03 and AU02; Figs. 4–7). The contamination moves, according to the direction of sedimentary transport and resuspension of the sediment in the water column, from the southern to the northern area. This transport is evident as the maximum concentration peak for Hg, Ba, HCB and PCB moves from deeper levels (in the southern area) to increasingly shallower levels in the northern one, according to the different sedimentation rates in the different sectors (Bellucci et al., 2012; Croudace et al., 2015). A second gradient, which starts from the southern sector and moves towards the central area, was recognised with an increase of concentrations of the main contaminants in the most superficial layers (AU08, AU07 and AU04; Figs. 4–7 and graphical abstract). The persistence of extremely high concentrations for all the contaminants at the core top of the southern source area in 2008, despite the closure of the chlor-alkali plant in 2003, indicates that some degree of sediment reworking and redistribution of contaminated sediment, at least in part driven by resuspension generated by shipping activities, must be occurring, representing an

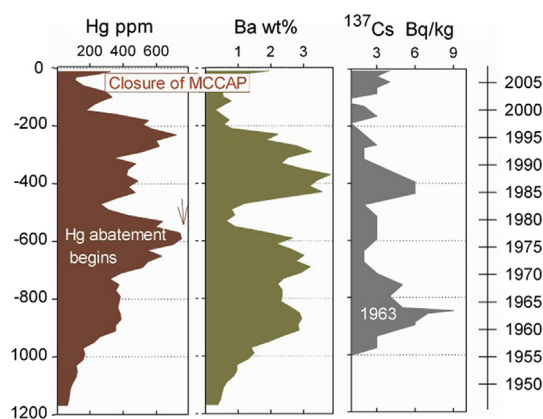


**Fig. 11.** Elemental profiles (Hg, Ba) determined by WD-XRF along the depth (cm) with chronology based on Cs-137 dating from a sediment core collected in the site AU10 (Croudace et al., 2015 modified).

environmental health concern. In particular, Hg contamination can persist in sediments over a long period, at risk of transformation into methyl-mercury (MeHg), which can bioaccumulate in organisms and biomagnify in the aquatic food chain (Ullrich et al., 2007). In addition, PCBs and HCB can persist for a very long time in sediments with high potential to be incorporated into the food web via benthic–pelagic coupling (Minh et al., 2007).

## 5.2. Sediment texture as a proxy of anthropogenic impact

The anthropogenic impact on coastal areas may not be limited to the supply of contaminants but may influence the natural sedimentation due to land use, alteration of natural coastline, construction of facilities, and other factors (De Falco et al., 2004; A. Wang et al., 2020). In this research, the coupled study of textural and chemical variations of the sediments was applied to reconstruct the industrial impact occurred in the marine area. Grain size and chemical variations throughout the cores are distinct and clearly indicated (e.g. Fig. 10). In the PCA scatter plot, silt and clay are positioned on positive values of PC2, while sand aligns on negative values; greater homogeneity is recognisable from the narrow PC2 range for cores AU01, AU02 and AU04, entirely correlated with higher clay contents, and AU05 and AU08, characterised by a lower content of fine fractions relative to the previous ones (Fig. 9). By contrast, AU03, AU06, AU09 and AU10 showed a very wide range of PC2 values, corresponding to high textural variability. Considering the plot of sediment particle size distribution with depth (Fig. 2), it was observed that, for AU03, AU09 and AU10, textural changes characterised the whole core length, and were interpreted as anthropogenic influences as they are closely located to industrial jetties. This fact was confirmed by the anthropogenic elements recognised by the qualitative mineralogical study (Fig. 3). In the scatter plot of AU06 were 2 distinct groups of samples, one with negative values of PC2, associated with higher sand contents, and another one in the positive side, correlated with higher silt and clay. Observing the vertical distribution of the pelitic fraction with respect to the contaminant concentration profiles (Fig. 12), it is clear that this distribution in the PCA corresponds to coarser sedimentation, associated to unpolluted sediments, in the lower core section and an increase of finer fractions in the upper one, with textural change occurring at approximately –50 cm, in concurrence with the first increase of contaminants. This change coincides

with the construction of the breakwater dams that closed the bay in the early 1960s, favouring the isolation and deposition of finer sediments as well as associated contaminants. Considering that the chlor-alkali plant started operations in 1958, and that the sampling resolution of cores and sedimentation rates in the central sector of the harbour range from 10 to 13 mm yr<sup>-1</sup> (Bellucci et al., 2012; Croudace et al., 2015), this event was coincident (Fig. 12). Although other processes could be considered as possible causes of such textural change (e.g. bioturbation, storms or vessel activity), it is unlikely that any could lead to many tens of centimetres of accumulation of finer sediment above dominantly coarser ones (Giangrande et al., 2002; Bennington and Farmer, 2015).

Regarding bioturbation, no evidence of burrowing activity was recognised during core subsampling. At the same time, the effect of storm events should consist of distinct high energy layers (increased grain size) repeated in the core record with erosional surfaces at the base (Saito, 1989). A total of 12 anomalous layers, characterised by increased grain size and supply of allochthonous foraminiferal fauna, were recognised in the sedimentary record of cores collected offshore from Augusta Bay. Some of these layers were correlated to historical tsunamis, the most recent one in 1908 (Smedile et al., 2011). Then, a change in sedimentation conditions which could favour the settlement of fine particles occurred at a certain time and is still occurring today, attributed to the establishment of a breakwater in the early 1960s. This event is therefore inferred to coincide with the start of contamination.

## 6. Conclusion

Over the last decade, sediment contamination in Augusta Harbour has been the focus of several environmental studies that recognised the exceptionally high anthropogenic disturbance of sediments by Hg, Ba, PCBs and HCB in the southernmost sector. Based on location, chemical characteristics, spatial distribution and chronology of pollution events, it has been possible to identify the pollution sources. These indicate pollution derived from the operation of the former chlor-alkali plant and inputs from nearby petrochemical plants. The earlier studies focused on specific cases while the present work has considered a broader dataset, obtained from 10 sediment cores distributed across the whole harbour area. This design allowed for the assessment of detailed information on spatial and vertical contamination patterns and

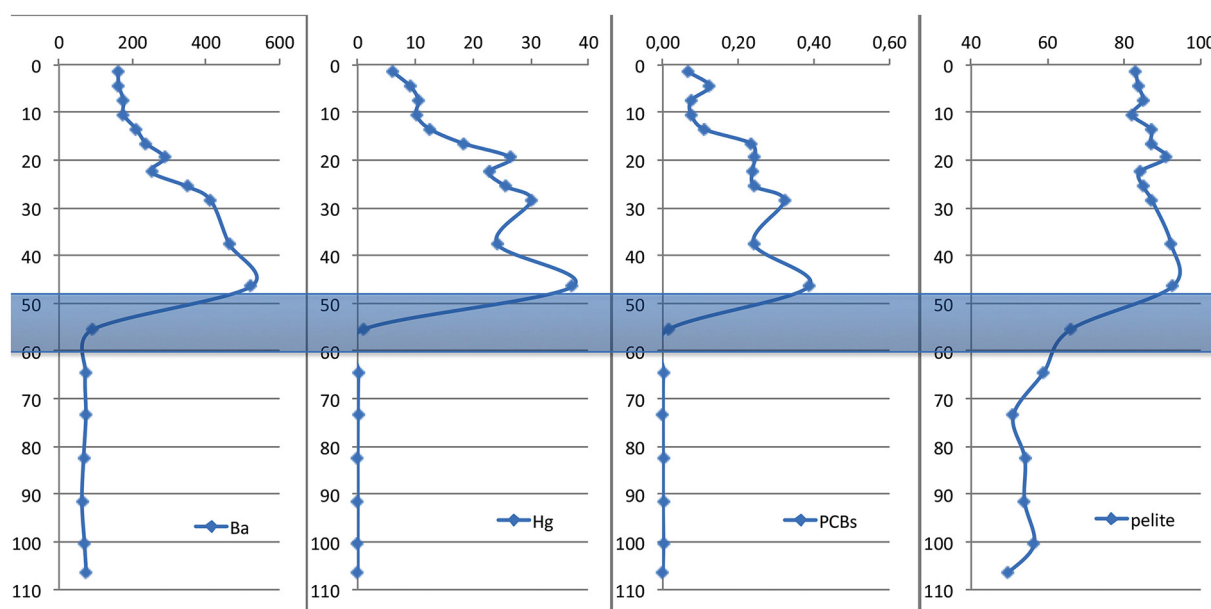


**Fig. 12.** Comparison among concentration profiles (mg kg<sup>-1</sup>) and pelitic fraction (%) along the depth (cm) in AU06 core. The bar represents the depth range corresponding to 1960, according to the sedimentation rates determined by Bellucci et al. (2012) and Croudace et al. (2015).

further evidence on the source of contamination to understand the broader context of pollution. An integrated approach that considered textural and chemical characteristics of sediments to indicate the anthropogenic impact was used to determine contaminant origin and to infer pollution transport dynamics.

The main findings of the present research are

- a highly contaminated sector in the southernmost area acts as a secondary source of contamination through reworking, resuspension and transport;
- patterns of contamination in the whole harbour area are caused by redistribution of contaminated sediments from the secondary source area;
- a contaminant-trap effect exists in the central sector of the harbour associated with increased fine sedimentation inputs linked to the enclosure of the bay.

This study shows that Augusta Harbour sediment cores record valuable environmental information. In particular, it has been demonstrated how the variations of the textural characteristics recognised in sediment cores are determined by the changes in the sedimentary environment caused by anthropogenic activities, and how these reflect the distribution of contamination in the whole area. A recommendation arising from this research is that the sedimentological investigation should always be considered in association with chemical studies, not merely for the assessment of contamination levels, but as a reliable proxy of anthropogenic impact, as well as the chemical signature, especially in enclosed areas affected by historical contamination.

## CRediT authorship contribution statement

**E. Romano:** Conceptualization, Methodology, Investigation, Writing - original draft, Writing - review & editing. **L. Bergamin:** Formal analysis, Writing - original draft, Visualization, Writing - review & editing. **I.W. Croudace:** Investigation, Supervision, Writing - review & editing. **G. Pierfranceschi:** Data curation, Methodology. **G. Sesta:** Data curation, Methodology. **A. Ausili:** Conceptualization, Investigation, Supervision, Writing - review & editing.

## Declaration of competing interest

The authors declare that they have no known competing financial interests or personal relationships that could have appeared to influence the work reported in this paper.

## Acknowledgements

The authors are grateful to Maria Celia Magno and Francesco Venti for grain size analysis and to Chiara Maggi for heavy metal analyses; besides, to Andrea Salmeri for supporting the drawing of georeferenced maps.

## Appendix A. Supplementary data

Supplementary data to this article can be found online at <https://doi.org/10.1016/j.scitotenv.2020.142683>.

## References

Apitz, S.E., Degetto, S., Cantaluppi, C., 2009. The use of statistical methods to separate natural background and anthropogenic concentrations of trace elements in radiochronologically selected surface sediments of the Venice Lagoon. *Mar. Pollut. Bull.* 58, 402–414. <https://doi.org/10.1016/j.marpolbul.2008.10.007>.

Ausili, A., Gabellini, M., Cammarata, G., Fattorini, D., Benedetti, M., Pisanelli, B., Gorbi, S., Regoli, F., 2008. Ecotoxicological and human health risk in a petrochemical district of southern Italy. *Mar. Environ. Res.* 66, 215–217. <https://doi.org/10.1016/j.marenvres.2008.02.062>.

Ausili, A., Bergamin, L., Romano, E., 2020. Environmental status of Italian coastal marine areas affected by long history of contamination. *Front. Environ. Sci.* 8, 34. <https://doi.org/10.3389/fenvs.2020.00034>.

Bellucci, L.G., Giuliani, S., Romano, S., Albertazzi, S., Mugnai, C., Frignani, M., 2012. An integrated approach to the assessment of pollutant delivery chronologies to impacted areas: Hg in the Augusta Bay (Italy). *Environ. Sci. Technol.* 46, 2040–2046. <https://doi.org/10.1021/es203054c>.

Benmoussa, T., Amrouni, O., Dezileau, L., Mahé, G., Saâdi, A., 2018. The sedimentological changes caused by human impact at the artificial channel of Medjerda-River (Coastal zone of Medjerda, Tunisia). *Proc. IAHS* 377, 77–81. <https://doi.org/10.5194/piahs-377-77-2018>.

Bennington, J.B., Farmer, C., 2015. Recognizing past storm events in sediment cores based on comparison to recent overwash sediments deposited by superstorm sandy. In: Bennington, J.B., Farmer, C. (Eds.), *Learning from the Impacts of Superstorm Sandy*. Academic Press.

Bergamin, L., Romano, E., Finoia, M.G., Venti, F., Bianchi, J., Colasanti, A., Ausili, A., 2009. Benthic foraminifera from the coastal zone of Baia (Naples, Italy): assemblage distribution and modification as tools for environmental characterisation. *Mar. Pollut. Bull.* 59, 234–244. <https://doi.org/10.1016/j.marpolbul.2009.09.015>.

Birch, G.F., 2016. Determination of sediment metal background concentrations and enrichment in marine environments - a critical review. *Sci. Total Environ.* 580, 813–831. <https://doi.org/10.1016/j.scitotenv.2016.12.028>.

Bonsignore, M., Salvaggio Manta, D., Oliveri, E., Sprovieri, M., Basilone, G., Bonanno, A., Falco, F., Traina, A., Mazzola, S., 2013. Mercury in fishes from Augusta Bay (southern Italy): risk assessment and health implication. *Food Chem. Toxicol.* 56, 184–194. <https://doi.org/10.1016/j.fct.2013.02.025>.

Buckley, D.E., Smith, J.N., Winters, G.V., 1995. Accumulation of contaminant metals in marine sediments of Halifax Harbour, Nova Scotia: environmental factors and historical trends. *Appl. Geochem.* 10 (2), 175–195.

Carbone, S., 2011. Note illustrative della Carta Geologica d'Italia alla scala 1:50.000 - Foglio 641 Augusta. Servizio Geologico d'Italia (247 pp).

Chen, C.F., Ju, Y.R., Chen, C.W., Dong, C.D., 2016. Vertical profile, contamination assessment, and source apportionment of heavy metals in sediment cores of Kaohsiung Harbor, Taiwan. *Chemosphere* 165, 67–79. <https://doi.org/10.1016/j.chemosphere.2016.09.019>.

Covelli, S., Fontolan, G., Faganeli, J., Ogrinc, N., 2006. Anthropogenic markers in the Holocene stratigraphic sequence of the Gulf of Trieste (northern Adriatic Sea). *Mar. Geol.* 230, 29–51. <https://doi.org/10.1016/j.margeo.2006.03.013>.

Crain, C.M., Halpern, B.S., Beck, M.W., Kappel, C.V., 2009. Understanding and managing human threats to the coastal marine environment. In: *The Year in Ecology and Conservation Biology, 2009*. Ann. N.Y. Acad. Sci. 1162, 39–62. <https://doi.org/10.1111/j.1749-6632.2009.04496.x>.

Croudace, I.W., Romano, E., Ausili, A., Bergamin, L., Rothwell, G., 2015. X-ray core scanners as an environmental forensic tool: a case study of polluted harbor sediment (Augusta Bay, Sicily). In: Croudace, I.W., Rothwell, R.G. (Eds.), *Micro-XRF Studies of Sediment Cores*. Springer, pp. 393–421. [https://doi.org/10.1007/978-94-017-9849-5\\_15](https://doi.org/10.1007/978-94-017-9849-5_15).

De Falco, G., Magni, P., Teräsuvuori, L.M.H., Matteucci, G., 2004. Sediment grain size and organic carbon distribution in the Cabras Lagoon (Sardinia, Western Mediterranean). *Chem. Ecol.* 20 (1), 367–377. <https://doi.org/10.1080/02757540310001629189>.

Di Leonardo, R., Mazzola, A., Tramati, C.D., Vaccaro, A., Vizzini, S., 2014. Highly contaminated areas as sources of pollution for adjoining ecosystems: the case of Augusta Bay (Central Mediterranean). *Mar. Pollut. Bull.* 89 (1–2), 417–426.

Feola, A., Lisi, I., Salmeri, A., Venti, F., Pedroncini, A., Gabellini, M., Romano, E., 2016. Platform of integrated tools to support environmental studies and management of dredging activities. *J. Environ. Manag.* 166, 357–373. <https://doi.org/10.1016/j.jenvman.2015.10.022>.

Gao, W., Du, Y., Gao, S., Ingels, J., Wang, D., 2016. Heavy metal accumulation reflecting natural sedimentary processes and anthropogenic activities in two contrasting coastal wetland ecosystems, eastern China. *J. Soils Sediments* 16, 1093–1108. <https://doi.org/10.1007/s11368-015-1314-0>.

Garron, C., Gagné, F., Ernst, W., Julien, G., Bernier, M., Caldwell, C., 2005. Mercury contamination of marine sediments and blue mussels (*Mytilus edulis*) in the vicinity of a mercury cell chlor-alkali plant in Dalhousie, New Brunswick, Canada. *Water Qual. Res. J. Canada* 40 (1), 1–15.

Giangrande, A., Montresor, M., Cavallo, A., Licciano, M., 2002. Influence of *Naineris laevigata* (Polychaeta: Orbiniidae) on vertical grain size distribution, and dinoflagellate resting stages in the sediment. *J. Sea Res.* 47, 97–108.

Hammer, Ø., Harper, D.A.T., Ryan, P.D., 2001. PAST: paleontological statistic software package for education and data analysis. *Palaeontologia Electronica* 4 (1), 9 (178 kb).

Huerta-Díaz, M.A., Delgadillo-Hinojosa, F., Hernandez-Ayon, M., Segovia-Zavala, J.A., García-Esquivel, Z., Lopez-Zarate, H., Siqueiros-Valencia, A., Galindo-Bect, S., 2008. Diagnosis of trace metal contamination in sediments: the example of Ensenada and El Sauzal, two harbours in Baja California, Mexico. *Mar. Environ. Res.* 66, 345–358. <https://doi.org/10.1016/j.marenvres.2008.05.008>.

ICRAM, 2008. Progetto preliminare di bonifica della Rada di Augusta inclusa nel sito di bonifica di interesse nazionale di Priolo. Fase I e II. Elaborazione definitiva. Technical report (253 pp).

Lisi, I., Taramelli, A., Di Risio, M., Cappucci, S., Gabellini, M., 2009. Flushing efficiency of Augusta harbour (Italy). *J. Coast. Res.* SI 56, 841e845.

Magagnoli, A., Mengoli, M., 1995. Carotiere a gravità SW-104 per carote di sedimento e acqua di fondo di grande diametro e minimo disturbo. Rapporto Tecnico IGM 27 (45 pp).

Matschullat, J., Ottestein, R., Reiman, C., 2000. Geochemical background - can we calculate it? *Environ. Geol.* 39, 990–1000. <https://doi.org/10.1007/s002549900084>.

Minh, N.H., Minh, T.B., Kajiwar, N., Kunisue, T., Iwata, H., Viet, P.H., Cam Tu, N.P., Tuyen, B.C., Tanabe, S., 2007. Pollution sources and occurrences of selected persistent organic pollutants (POPs) in sediments of the Mekong River delta, South Vietnam. *Chemosphere* 67, 1794–1801. <https://doi.org/10.1016/j.chemosphere.2006.05.144>.

Moon, H.B., Choi, M., Choi, H.G., Ok, G., Kannan, K., 2009. Historical trends of PCDDs, PCDFs, dioxin-like PCBs and nonylphenols in dated sediment cores from a semi-

- enclosed bay in Korea: tracking the sources. *Chemosphere* 75 (5), 565–571. <https://doi.org/10.1016/j.chemosphere.2009.01.064>.
- Muthu Raj, S., Jayaprakash, M., 2008. Distribution and enrichment of trace metals in marine sediments of Bay of Bengal, off Ennore, southeast coast of India. *Environ. Geol.* 56 (1), 207–217. <https://doi.org/10.1007/s00254-007-1156-1>.
- Ontiveros-Cuadras, J.F., Ruiz-Fernández, A.C., Pérez-Bernal, L.H., Serrato de la Peña, J.L., Sanchez-Cabeza, J.A., 2019. Recent trace metal enrichment and sediment quality assessment in an anthropized coastal lagoon (SE gulf of California) from  $^{210}\text{Pb}$ -dated sediment cores. *Mar. Pollut. Bull.* 149, 110653. <https://doi.org/10.1016/j.marpolbul.2019.110653>.
- Owen, R.B., Sandhu, N., 2000. Heavy metal accumulation and anthropogenic impacts on Tolo Harbour, Hong Kong. *Mar. Poll. Bull.* 40 (2), 174–180. [https://doi.org/10.1016/S0025-326X\(99\)00201-5](https://doi.org/10.1016/S0025-326X(99)00201-5).
- Reynoldson, T.B., 1987. Ecological effects of in situ sediment contaminants. In: Thomas, R., Evans, R., Hamilton, A., Munawar, M., Reynoldson, T., Sadar, H. (Eds.), *Ecological Effects of In Situ Sediment Contaminants*. Hydrobiologia vol. 149, pp. 53–66.
- Rodenburg, L.A., Ralston, D.K., 2017. Historical sources of polychlorinated biphenyls to the sediment of the New York/New Jersey Harbor. *Chemosphere* 169, 450–459. <https://doi.org/10.1016/j.chemosphere.2016.11.096>.
- Romano, E., Bergamin, L., Fioia, M.G., Celia Magno, M., Mercatali, I., Ausili, A., Gabellini, M., 2009. The effects of human impact on benthic foraminifera in the Augusta Harbour (Sicily, Italy). In: Moksness, E., Dahl, E., Støttrup, J. (Eds.), *Integrated Coastal Zone Management*. Wiley-Blackwell, pp. 97–115.
- Romano, E., Bergamin, L., Celia Magno, M., Ausili, A., 2013. Sediment characterization of the highly impacted Augusta harbour (Sicily, Italy): modern benthic foraminifera in relation to grain-size and sediment geochemistry. *Environ. Sci.-Proc. Imp.* 15, 930–946. <https://doi.org/10.1039/C3EM30824C>.
- Romano, E., Bergamin, L., Croudace, I.W., Ausili, A., Maggi, C., Gabellini, M., 2015. Establishing geochemical background levels of selected trace elements in areas having geochemical anomalies: the case study of the Orbetello lagoon (Tuscany, Italy). *Environ. Pollut.* 202, 96–103. <https://doi.org/10.1016/j.envpol.2015.03.017>.
- Romano, E., Bergamin, L., Ausili, A., Celia Magno, M., Gabellini, M., 2016. Evolution of the anthropogenic impact in the Augusta Harbor (Eastern Sicily, Italy) in the last decades: benthic foraminifera as indicators of environmental status. *Environ. Sci. Pollut. Res.* 23 (11), 10514–10528. <https://doi.org/10.1007/s11356-015-5783-x>.
- Romano, E., Bergamin, L., Celia Magno, M., Ausili, A., Gabellini, M., Croudace, I.W., 2018a. Differences in acquisition of environmental data in strongly impacted marine sediments using gravity and vibro corers: the case-study of Augusta harbor (Eastern Sicily, Italy). *Measurement* 124, 184–190. <https://doi.org/10.1016/j.measurement.2018.04.025>.
- Romano, E., Celia Magno, M., Bergamin, L., 2018b. Grain size of marine sediments in the environmental studies from sampling to measuring and classifying. A critical review of the most used procedures. *Acta IMEKO* 7 (2), 10–15. [https://doi.org/10.21014/acta\\_imeko.v7i2.537](https://doi.org/10.21014/acta_imeko.v7i2.537).
- Ruiz-Fernández, A.C., Rangel-García, M., Pérez-Bernal, L.H., López-Mendoza, P.G., Gracia, A., Schwing, P., Hollander, D., Páez-Osuna, F., Cardoso-Mohedano, J.G., Cuellar-Martínez, T., Sanchez-Cabeza, J.A., 2019. Mercury in sediment cores from the southern Gulf of Mexico: preindustrial levels and temporal enrichment trends. *Mar. Pollut. Bull.* 149, 110498. <https://doi.org/10.1016/j.marpolbul.2019.110498>.
- Saito, Y., 1989. Modern storm deposits in the inner shelf and their recurrence intervals, Sendai Bay, northeastern Japan. In: Taira, A., Masuda, F. (Eds.), *Sedimentary Facies in the Active Plate Margin*. Terra Scientific Publishing Company, Tokyo, pp. 331–344.
- Salomons, W., de Rooij, N.M., Kerdijs, H., Bril, J., 1987. Sediments as a source for contaminants? In: Thomas, R., Evans, R., Hamilton, A., Munawar, M., Reynoldson, T., Sadar, H. (Eds.), *Ecological Effects of in Situ Sediment Contaminants*. Hydrobiologia vol. 149, pp. 13–30.
- Salvagio Manta, D., Bonsignore, M., Oliveri, E., Barra, M., Tranchida, G., Giaramita, L., Mazzola, S., Sprovieri, M., 2016. Fluxes and the mass balance of mercury in Augusta Bay (Sicily, southern Italy). *Estuar. Coast. Shelf Sci.* 18, 134–143. <https://doi.org/10.1016/j.ecss.2016.08.013>.
- Sciaccia, S., Fallico, R., 1978. Presenza e concentrazione di sostanze inquinanti di origine industriale nella Rada di Augusta (Siracusa). *Inquinamento* 20 (6), 33–38.
- Shen, F., Mao, L., Sun, R., Du, J., Tan, Z., Ding, M., 2019. Contamination evaluation and source identification of heavy metals in the sediments from the Lishui River Watershed, Southern China. *Int. J. Environ. Res. Public Health* 16, 336. <https://doi.org/10.3390/ijerph16030336>.
- Shepard, F.P., 1954. Nomenclature based on sand-silt-clay ratios. *J. Sediment. Petrol.* 24, 151–158.
- Signa, G., Mazzola, A., Doriana Tramati, C., Vizzini, S., 2017. Diet and habitat use influence Hg and Cd transfer to fish and consequent biomagnification in a highly contaminated area: Augusta Bay (Mediterranean Sea). *Environ. Pollut.* 230, 394–404. <https://doi.org/10.1016/j.envpol.2017.06.027>.
- Smedile, A., De Martini, P.M., Pantosti, D., Bellucci, L., Del Carlo, P., Gasperini, L., Pirrotta, C., Polonia, A., Boschi, E., 2011. Possible tsunami signatures from an integrated study in the Augusta Bay offshore (Eastern Sicily-Italy). *Mar. Geol.* 281, 1–13.
- Sprovieri, M., Oliveri, E., Di Leonardo, R., Romano, E., Ausili, A., Gabellini, M., Saggiomo, V., Barra, M., Tranchida, G., Bellanca, A., Neri, R., Budillon, F., Mazzola, S., 2011. The key role played by the Augusta basin (southern Italy) in the mercury contamination of the Mediterranean Sea. *J. Environ. Monit.* 13, 1753–1760. <https://doi.org/10.1039/c0em00793e>.
- Tamburrino, S., Passaro, S., Salvagio Manta, D., Quinci, E., Ausili, A., Romano, E., Sprovieri, M., 2020. Re-shaping the “original SIN”: a need to re-think sediment management and policy by introducing the “buffer zone” concept. *J. Soils Sediments* 20, 2563–2572. <https://doi.org/10.1007/s11368-019-02486-1>.
- Tang, C.W., Ip, C.C., Zhang, G., Shin, P.K.S., Qian, P., Li, X., 2008. The spatial and temporal distribution of heavy metals in sediments of Victoria Harbour, Hong Kong. *Mar. Pollut. Bull.* 57, 816–825. <https://doi.org/10.1016/j.marpolbul.2008.01.027>.
- Tanner, P.A., Leong, L.S., Pan, S.M., 2000. Contamination of heavy metals in marine sediment cores from Victoria Harbour, Hong Kong. *Mar. Pollut. Bull.* 40, 769–779. [https://doi.org/10.1016/S0025-326X\(00\)00025-4](https://doi.org/10.1016/S0025-326X(00)00025-4).
- Tessier, A., Campbell, P.G.C., 1988. Partitioning of trace metals in sediments. In: Kramer, J.R., Allen, H.E. (Eds.), *Metal Speciation: Theory Analysis and Application*. 183–199. Lewis publisher.
- Tomlinson, D.L., Wilson, J.G., Harris, C.R., Jeffrey, D.W., 1980. Problems in the assessment of heavy-metal levels in estuaries and the formation of a pollution index. *Helgolander Meeresunters.* 33, 566–575.
- Ullrich, S.M., Ilyushchenko, M.A., Tanton, T.W., Uskov, G.A., 2007. Mercury contamination in the vicinity of a derelict chlor-alkali plant part II: contamination of the aquatic and terrestrial food chain and potential risks to the local population. *Sci. Total Environ.* 381, 290–306. <https://doi.org/10.1016/j.scitotenv.2008.10.065>.
- Wang, A., Ye, X., Lin, Z., Wang, L., Lin, J., 2020a. Response of sedimentation processes in the Minjiang River subaqueous delta to anthropogenic activities in the river basin. *Estuar. Coast. Shelf Sci.* 232, 106484. <https://doi.org/10.1016/j.ecss.2019.106484>.
- Wang, R., Zhang, C., Huang, X., Zhao, L., Yang, S., Struck, U., Yin, D., 2020b. Distribution and source of heavy metals in the sediments of the coastal East China sea: geochemical controls and typhoon impact. *Environ. Pollut.* 260, 113936. <https://doi.org/10.1016/j.envpol.2020.113936>.
- WHO, 2012. Biomonitoring-based indicators of exposure to chemical pollutants. Report of a meeting Catania, Italy, 19–20 April 2012, WHO Report (Europe). Regional Office for Europe, Copenhagen, Denmark.
- Yang, G., Song, Z., Sun, X., Chen, C., Ke, S., Zhang, J., 2020. Heavy metals of sediment cores in Dachen Bay and their responses to human activities. *Mar. Pollut. Bull.* 150, 110764. <https://doi.org/10.1016/j.marpolbul.2019.110764>.
- Zhou, F., Guo, H., Liu, L., 2007. Quantitative identification and source apportionment of anthropogenic heavy metals in marine sediment of Hong Kong. *Environ. Geol.* 53, 295–305. <https://doi.org/10.1007/s00254-007-0644-7>.
- Zourarah, B., Maanan, M., Carruesco, C., Aajjane, A., Mehdi, K., Conceição Freitas, M., 2007. Fifty-year sedimentary record of heavy metal pollution in the lagoon of Qualidia (Moroccan Atlantic coast). *Estuar. Coast. Shelf Sci.* 72 (1–2), 359–369. <https://doi.org/10.1016/j.ecss.2006.11.007>.